RSC Advances

ROYAL SOCIETY OF CHEMISTRY

www.rsc.org/advances

Effect of graphene modified by ionic liquid with long alkyl chain on crystallization kinetics behavior of poly(vinylidene fluoride)

Yadong Hu, Pei Xu*, Haoguan Gui, Shanzhong Yang,Yunsheng Ding*

Key Laboratory of Advanced Functional Materials and Devices, Anhui Province, Department of Polymer Material and Engineering, School of Chemistry and Chemical Engineering, Hefei University of Technology, Hefei 230009, P.R. China.

To investigate the effects of graphene (Gra) modified by a long alkyl chain ionic liquid (1-hexadecyl-3-methylimidazolium bromide, IL) on the crystallization kinetics behaviour of poly(vinylidene fluoride) (PVDF), a series of PVDF/IL blend, PVDF/Gra and PVDF/IL/Gra nanocomposites have been prepared using solution-cast method. The crystallization kinetics and corresponding crystal structure have been investigated using differential scanning calorimetry (DSC), polarized optical microscopy (POM) and X-ray diffraction spectra (XRD). Crystallization kinetic parameters, such as relative crystallinity (X_t), crystallization half time ($t_{1/2}$), crystallization rate constant (Z), Avrami exponents (n) and activation energy (E_a) have been determined by both isothermal and non-isothermal techniques. In the isothermal and non-isothermal crystallization process, for PVDF/0.5IL/0.5Gra, IL and Gra can facilitate nucleation to decrease E_a, synergistic efforts of the IL and Gra can maintain appropriate crystallization rate to form β phase extruded form α phase. The positive effect on the crystallization of PVDF may be ascribed to not only due to the existence of Gra-cation interaction between the imidazolium cation and the aromatic carbon ring structure, but also due to the electrostatic interaction between the $>CF_2$ group of the polymer backbone and imidazolium cation.

1. Introduction

Poly(vinylidene fluoride) (PVDF) has attracted more and more attention as one of the most important

Corresponding author. Tel.: +86 551 62901545.

E-mai addresses: chxuper@ hfut.edu.cn (P. Xu), dingys@hfut.edu.cn (Y. Ding),.

semi-crystalline polymers because of its good thermal stability, chemical resistance, mechanical and electrical properties.[1-3] There are several kinds of crystal phase types (α, β, γ and δ) of PVDF, and unique piezoelectric and pyroelectric performance of PVDF closely relate to the polar crystal phase.[4-9] Normally, among them the α phase can be easily obtained from melt crystallization, showing non-polar with TGTG chain conformation, while the rest of crystal phase have polarity. The β and γ phase have an orthorhombic unit cell with TTTT and TTTG chain conformation, respectively, and the structure of β phase results in the most polar PVDF.[10] Thus, the appearance of β phase can expand the application filed of PVDF as capacitors, actuators, piezoelectric and pyroelectric sensors, and power cable terminations. The oriented or un-oriented β-crystal can be obtained from melt under specific conditions, such as external electric field, ultra-fast cooling from solution crystallization at temperatures below 70 ºC, by mechanical stretching of the α-PVDF and the addition of nucleating fillers (such as clay, $BaTiO_3$, TiO_2, and hydrated ionic salt).[10,11] The physical processes of promoting the β-PVDF content are rigorous such as high pressure and high certain temperature, and the nanofillers will have major influences of mechanical properties when they are most in the matrix as inducer. Based on these, the ionic liquid (IL) with ions and graphene (Gra) with rigid structure are selected to enhance the polar phase content and perfect the crystallization behavior.

IL is a room temperature molten salt with a bulky organic cation and inorganic anion, exhibiting apparent non-flammability, low viscosity, good electrical conductivity, high thermal and air stability and low vapor pressure.[12, 13] Thus, it is deemed to "Green" additive in a variety of research filed, such as crystallization,[14] flame retardant system,[15] toughened system, high dielectric constant system[16] and so on. He et al. found a facile and effective method to enhance the content of β phase in PVDF via incorporating with different types of ILs because of "ion-dipole" interaction.[17] Liang et al. investigated the effect of content of cetyl trimethyl ammonium bromide and isothermal crystallization temperature on the content of polar phase.[18] Xing et al. combined the different contents of $[BMIm]PF_6$ and PVDF, the γ phase has been induced successfully.[19, 20] There is an electrostatic interaction between imidazolium ions and $>CF_2$ groups of PVDF, which was characterized by FTIR. Okada said that PVDF particles were partly transformed into β phase PVDF by adding $[BMIm]NO_3$ and subsequent thermal annealing just below the melting point of the PVDF/IL blends.[21]

Gra consists of a monolayer of sp^2 bonded carbon atoms, which has large aspect ratio and leading to the strong interaction between polymer matrix and Gra.[22, 23] Some investigations have pointed out the

excellent mechanical and electric properties of polymer/Gra system. Gra was used to as nucleating agent during the crystallization of semicrystalline polymers by many researchers. Layek and An et al. prepared the PVDF/Gra composites and found the Gra can result in phase transformation from α to β PVDF.[24-26] Han found the reflection strengths of polar phase in XRD results were generally influenced by the reduced graphene (RG) content in the PVDF/RG nanocomposite.[27] Huang added only 0.05 *wt* % of GO can partially transform the α phase to β phase in PVDF/rGO system.[28] Based on the above conclusions, Gra may have a good effect for improving the content of polar crystals in PVDF systems.

Compared with other methods of modified Gra, the use of IL has the following advantages: first, the cation-π physical interactions between IL and Gra is strong, which can maintain the excellent physical properties of Gra;[29-31] secondly, this method is simple, environmentally friendly, and has a relatively high efficiency.[32, 33] Inspired by the above benefits, the imidazolium ionic liquid was used as a coupling agent between the Gra and poly(methyl methacrylate) (PMMA) by solution formation and in situ polymerization method, to promote the dispersibility of Gra and increase the conductivity of the composites.[34]

There are two successive events: the primary nucleation of a new phase from the melt polymer and then the three-dimensional growth.[6, 35] Most recently, the use of the imidazolium ionic liquids with long alkyl chain ([C_{16}MIm]Br) and Gra as the fillers for modifying PVDF has focused primarily on the crystal structure and crystallization behavior. This article introduces the preparation of PVDF/IL, PVDF/Gra and PVDF/IL/Gra composite films and the crystal structure which is characterized by XRD, POM and the melting/cooling curves of DSC. And the nucleation and growth mechanism will be changed because of the presence of new crystal. So the Avrami equation is proposed to study the isothermal crystallization kinetics and its other form is used to calculate the energy contrast. The Avrami equation and Flynn-Wall-Ozawa methods were used for investigating the non-isothermal crystallization kinetics, and Flynn-Wall-Ozawa method is an isoconversional method without considering the process. The differences of crystals will have a big fall in crystallization parameters and kinetics.

The key point of this work is to investigate the effects of IL with long alkyl chain and Gra with the rigid sheet structure on the crystal form and crystallization kinetics, which are worked as template agents. And the relationship between crystal form and kinetic parameters can be established, the interaction between nanoparticle, imidazolium salt and PVDF chain can be understood, finally, a proper

method to character and control of PVDF crystal can be provided.

2. Experimental

2.1 Materials

In this work, the utilized PVDF was purchased from Shanghai 3F New Material Co., China with a weight average molecular mass (M_w) of 2.2 × 10^5 g/mol and a polydispersity index of 2. The IL, 1-hexadecyl-3-methylimidazolium bromide, *i.e.* [C_{16}mim]Br, was obtained from Lanzhou Greenchem ILs, China and used as received. Gra (0.5-2 μm in diameter, 0.8-1.2 nm thickness) was obtained from Nanjing XFNANO Materials Tech Co., Ltd.

2.2 Sample Preparation

In order to avoiding the side effect of other matter, such as monomers, catalyst and other additives during its polymerization, the obtained PVDF was dissolved in N,N'-dimethyl formamide (DMF) as the solvent and then precipitated with methanol (MeOH). Then it was dried in an air drying oven at 60 °C for 4 h and a vacuum drying oven at 60 °C for 24 h.

The PVDF/1IL (99 *wt*% 1 *wt*%) blend, PVDF/1Gra (99 *wt*% 1 *wt*%) or PVDF/0.5IL/0.5Gra (99 *wt*% 0.5 *wt*% 0.5 *wt*%) composites were prepared as follows. Gra was dispersed in DMF by sonication. Then IL was added into the suspension under vigorous mechanical stirring at 80 °C for 1 h in order to form uniform slurry. At the same time, the washed PVDF was also dissolved in DMF. Then, the suspension of Gra or modified Gra in DMF was added to the PVDF solution, and the mixture was subjected to ultrasonic treatment for 10 min. Afterwards, the mixture was heated to 70 °C for 8 h to remove the solvent completely and molded by hot-pressing at 175 °C and 10 MPa subsequently. The voids can be removed by the hot-pressing process. Traces of water were removed by vacuum evaporation at room temperature for 24 h. The sample names and ratio of components are listed in Table 1. Structures of IL and schematic diagram of the preparation of PVDF/IL/Gra composite is shown in Fig. 1.

2.3 Differential Scanning Calorimetry (DSC)

Isothermal and non-isothermal crystallization kinetics measurements were finished by differential scanning calorimeter (DSC, 821e, Mettler Toledo). All the DSC samples were dried in vacuum drying oven at 40 °C for 12h and measurements were carried out in the nitrogen atmosphere. The sample weight was around 6 mg.

The isothermal run was carried out by heating from 25 °C to 200 °C at 50 °C/min and kept for 5min to eliminate thermal history, then cooled quickly at 50 °C/min to the predetermined crystallization temperature (T_c) and maintained for 30 min.

The non-isothermal crystallization kinetics were performed by first heating from 25 °C to 200 °C and maintained for 5 min to remove thermal history, then cooled to 0 °C at different rate of 2, 3, 5, 10 °C/min, respectively. Then, the samples were heated to 200 °C at 10 °C/min again and cooled to 0 °C at 50 °C/min. These curves are used to analyzing crystallization kinetics and melting behaviors.

2.4 Polarized Optical Microscopy (POM)

Samples were dissolved in DMF with the ratio of 1/10 g/mL, and the turbidity solution were dripped on a cover glass. The PVDF films were dried in vacuum dry oven at 60 °C for 12 h. Samples were heated to 200 °C for 5 min to remove thermal history on one hot stage, and transferred quickly to another hot stage at crystallization temperature which was set in advance under POM. This method was provided to observe the crystal morphology of PVDF and PVDF/1IL by POM.

2.5 X-ray Diffraction (XRD)

The crystal forms of samples were characterized by X'Port, PRO MPD, Holland. The machine was operated at a 40 kV voltage and 40 mA current. The data was recorded from 2θ = 5-30^o at a scanning speed of 2 ^{o}/min with a step interval of 0.02^o.

3. Result and Discussion

3.1 Isothermal Crystallization Kinetics.

Fig. 2 demonstrates the POM photos of neat PVDF and PVDF/IL crystallized at 147 ºC after banishing the thermal history. The spherulites with typical Maltese cross pattern have been observed in FVDF at 9 min and 30 min. With the addition of IL, the sample has crystallized completely at 9 min. It is quite clear that the number of spherulites with high birefringence in PVDF/IL is more than neat PVDF, and the nucleating effect of IL is observably. The movement of PVDF chain was limited during the molten stage because of the interaction between imidazole cations of ILs and >CF_2 groups of PVDF chain. The bottom right image of bright field can provide the evidence of crystallizing completely. So the polar phase co-existents with α-phase in the lower left image, which is darker and less birefringent spherulites. The size of α-crystal in PVDF/IL is small and irregular. The nucleus density and growth speed of polar phase is higher than α-crystal, and the space of growth crystal is finite, so the α-crystal

in PVDF/IL has been extruded by many small polar phases during the growth peocess.[36]

Fig. S1 shows the morphology of PVDF/1Gra and PVDF/1IL/1Gra. Fig. S2 records the process of isothermal crystallization of PVDF/1IL blend, PVDF/1Gra and PVDF/0.5IL/0.5Gra composites at the different predetermined crystallization temperature (T_c). Fig. S3 displays the relative crystallinity (X_t) versus time during isothermal crystallization of samples at different T_c.

At present, the well-known Avrami equation as follow was widely used to describe the nucleation and growth process in the study of overall crystallization kinetics.[37, 38]

$$X_t = 1 - \exp\left(-Zt^n\right) \qquad (1)$$

Where X_t is the relative degree of crystallinity at any time, Z is a rate constant related to nucleation and growth rate parameters, and n is called "Avrami exponent" which depends on the type of nucleation and the growth mechanism during the crystallization.[39] And one logarithmic form was given by eq. (2)

$$\log\left[-\ln\left(1 - X_t\right)\right] = \log Z + n \log t \qquad (2)$$

Generally, the plot of (log [-ln (1-X_t)]) versus (log t) can offer the straight line are represented in Fig. 3. We can calculate that slope of the line is n and the intercept with the ordinate yields (log Z). The half-time of crystallization ($t_{1/2}$) expresses the time needed to achieve 50% of crystallinity in this work to compare the overall crystallization rate, which could be calculated by the eq. (3) as follow:

$$t_{1/2} = \left(\ln 2 / Z\right)^{1/n} \qquad (3)$$

And the reciprocal of $t_{1/2}$ is the crystallization rate, G, eq. (4) as follow:

$$G = \tau_{1/2} = 1 / t_{1/2} \qquad (4)$$

The values of (log Z), n, and $t_{1/2}$ were represented in Table 2. The value of n, at different crystallization temperature, reflects 2D/3D crystal growth mechanism, which is commonly observed in a case of macromolecules. For neat PVDF, the Avrami exponent n is around 2.8 while in PVDF/IL blends and PVDF nanocomposites it is about 2.5, indicating that the presence of IL and Gra affected the crystallization mechanism of PVDF. For the same crystallization temperature, the n value decreases with increasing of Gra and IL filler concentration, indicating that the filler acts as nucleation agents during the primary crystallization process.[40] The POM images have observed several crystal types of PVDF/IL, which including α phase and others. So the mechanism of nucleating was changed.

For all samples the values of G that shows the crystallization rate decrease with the increase of T_c, indicating the decrease of the overall isothermal crystallization rate at higher crystallization temperatures. The nucleation becomes more difficult at higher crystallization temperatures, which reduces the overall crystallization rate.[39] It is observed that the crystallization rate of PVDF/1Gra or PVDF/0.5IL/0.5Gra was faster than that of PVDF at the same T_c, indicating that Gra can accelerate the isothermal crystallization process of the PVDF matrix greatly.[41] Compared with PVDF the value of G in PVDF/1IL firstly decreases and then increases with the increase of T_c, because the interaction between the $>CF_2$ group of PVDF chain and imidazolium cation of IL is stronger than the effect of plastification of IL to form β phase conformation firstly, and then the interaction between the $>CF_2$ group and imidazolium cation is weaker than the effect of plastification of IL with the increase of T_c. Compared with PVDF/1Gra the value of G in PVDF/0.5IL/0.5Gra decreases at the same T_c, because nucleation of Gra restrained the effect of plastification of IL, and β phase conformation can be formed because cationic imidazolium ring wrapped on the surface of Gra can induce PVDF to form the full zigzag conformations.[42]

The activation energy, E_a, can be calculated according to the Avrami equation as follow: [43]

$$(1/n)\ \ln Z = \ln Z_0 - \frac{1}{RT_C} E_a \qquad (5)$$

Where Z_0 is a temperature independent pre-exponential factor, E_a is the activation energy, R is the gas constant and T_c is the crystallization temperature. The Plot of $(1/n)$ $(\ln Z)$ versus $(1/T_c)$ of samples for the Avrami parameter K deduced from isothermal crystallization is shown in Fig. 4. It provides straight line with the slope is $(-E_a/R)$, then the E_a is calculated. The E_a are -592 KJ/mol, -400 KJ/mol, -336 KJ/mol and -364 KJ/mol for PVDF, PVDF/1Gra, and PVDF/0.5IL/0.5Gra, the negative means that process of crystallization is exothermal. In the isothermal crystallization process, IL and Gra can significantly support as nucleating agent at T_c to decrease the E_a for PVDF composites obviously, and IL and Gra can slightly restrain spherulitic growth at T_c to decrease the crystallization rate for PVDF composites slightly. An increase of the nucleation and a reduction of the spherulite growth rate result from a reduction of the crystallization time of composites. The value of E_a for PVDF/1Gra is the smallest because nucleating of Gra is stronger than that of IL. For PVDF/0.5IL/0.5Gra, IL and Gra can facilitate nucleation to decrease E_a, combined efforts of the IL and Gra can keep a specific value of G to form β phase extruded form α phase.

3.2 Non-Isothermal Crystallization Kinetics.

Fig. 5 shows DSC curves of all samples for the cooling process from 200 °C to 0 °C at 10 °C/min and 2 °C/min, the crystallization peak temperatures (T_p) of PVDF/IL blends is 1.3 °C lower than that of neat PVDF at high cooling temperature rate, and 1 °C higher than that of neat PVDF at low cooling temperature rate. This indicates the high cooling temperature rate and the existence of IL impede the motion of polymer chains at melting state.[44] The whole process of crystallization is associated with cooling temperate rate and the additive. The values of T_p shift to low temperature at the high cooling temperature rate, the reason is considered to be that cooling rate is faster than the motion of polymer segments or nucleation rate. When the cooling temperature rate is low, the IL acted as the nuclei of the polymer crystal. The molecular chains of the PVDF have enough time to move and the target of arrangement must be finished quickly due to the bigger nucleation density according to the photo of POM.[45] When Gra was dispersed into the matrix alone (PVDF/1Gra), the value of T_p slightly shift upon. With the Gra and IL (PVDF/0.5IL/0.5Gra) added, the value of T_p intensely shift upon, and the value of T_p is stronger than that of PVDF.

Gregorio and Cestari pointed out that different melting peak temperatures T_m matched the different phase of PVDF, and α-phase of PVDF melt at 167 °C.[46] According to Liang, the temperature range of 172-180 °C corresponds to β-PVDF or γ-PVDF. And γ-PVDF can be obtained from α-γ transition by melting at 189-190 °C.[18] Fig. 6 expresses the second heating DSC curves of all samples after cooling at 10 °C/min, respectively. The different T_m values are listed in Table. 3. The T_m of neat PVDF and PVDF/Gra is around 167 °C, this indicates that there is one type of crystal form in PVDF. But there are two melting peaks occur in samples which contains IL. The values of T_m of PVDF/1IL are 6 °C and 11 °C higher than that of PVDF, this means the different phase has been induced by 1 percentage of IL. In PVDF/0.5IL/0.5Gra, two peaks show α-PVDF co-existents with β-PVDF. Compared with PVDF/1IL, two T_m values in PVDF/0.5IL/0.5Gra decreases with the IL loading adding.

Fig. 7 displays the XRD profiles of samples. The different diffraction peaks are used to symbol the crystal phase. The α-phase of PVDF is located at $2\theta=17.4^o$, 18.2^o, 20.0^o and 26.2^o. β-phase presents a peak at $2\theta=20.2^o$, and γ-phase presents peaks at $2\theta=18.5^o$, 19.2^o and 20.04^o, respectively.[10] When IL was incorporated into the matrix alone (PVDF/1IL), the peak of β-phase slightly increased. With the Gra and IL (PVDF/0.5IL/0.5Gra) added, the peak of β-phase intensely increased, and the peak of α-phase is weaker than that of PVDF. And in PVDF/1Gra, a faint shoulder peak of β-phase appears. As

shown in this figure, the degree of crystallinity (χ) of the samples was evaluated by the intensity area ratio of the XRD peaks, each diffraction peak is separated into α-phase (red), β-phase (green) and amorphous phase (blue).[10, 21] According to the integrated intensity ratio of the diffraction peaks, χ of neat PVDF is estimated as 37%, the value corresponds well with that evaluated from the endothermic peak area in DSC trace of the neat PVDF. The enthalpy of fusion of PVDF is 35.9 J/ g and its perfect melting enthalpy is 104.6 J/g. Judging from the diffraction area ratio of each peak, mole fraction of β-phase crystal form was calculated as 9.2% for PVDF/IL, 1.3% for PVDF/Gra, 12.5% for PVDF/IL/Gra. The inductive effect of 1 percentage of IL is stronger than Gra, but the modified system is strongest among them. Thus, XRD result indicates the interaction between the $>CF_2$ group with the cation part in the IL can induce the polar phase in samples and the interaction between the $>CF_2$ group with IL wrapped on the Gra surface can strengthen the effect of induction, [47] but the interaction between PVDF chain and aromatic carbon ring is weak, which results in the bad inductive effect. Concluding from the above discussion, the IL is considered as a kind of inducers and the Gra is regarded as a nucleation agent for crystallization of composites.

Fig. S4, S5, and S6 show heat flow versus temperature, X_t versus temperature, and X_t versus time in the process of non-isothermal crystallization for samples, respectively. There are serval methods to describe the process of non-isothermal crystallization, the Avrami equation also can analyze as well as the process of isothermal crystallization. Jeziorny gave the modified Avrami equation as follow: [48]

$$X_t = 1 - \exp\left(-Z_t t^n\right) \quad \text{Or} \quad \log\left[-\ln\left(1 - X_t\right)\right] = \log Z_t + n \log t \qquad (6)$$

Where the Z_t is the crystallization rate constant related to the nucleation and growth mechanism. The values of Z_t and n were calculated from the slope and intercept of the straight region of the plot. Fig. 8 displays the plot of (log [-ln (1-X_t)]) versus (log t) for non-isothermal crystallization of samples. The range of X_t is 0.05-0.85. Considering the influence of cooling rate, Jeziorny suggested the value of Z_t should be modified using of cooling rate, the final form of equation was given as follow: [48]

$$\log Z_c = \frac{\log Z_t}{\Phi} \qquad (7)$$

The value of n, Z_c were got from Fig. 8, $t_{1/2}$ is listed in Table. 4. For neat PVDF, n is around 2.6, for other samples, the n is around 2.2, this change means the nucleation and growth mechanism are different.[39] Neat PVDF may have the dimensional spherulite during the process of crystallization, but the incomplete crystal was existence in the others. It is observed that the values of Z_c for PVDF/1Gra

and PVDF/0.5IL/0.5Gra are smaller than those of PVDF at the same cooling rate, meaning a much lower crystallization rate for PVDF in the composites. The growth rate decreases on increasing the content of IL or Gra for PVDF composites, but the IL or Gra, acting as nucleating sites, improve the nucleation ability for PVDF composites compared with PVDF. In the non-isothermal crystallization process, IL and Gra can support nucleating agent at higher temperature, but IL and Gra can restrain spherulitic growth at lower temperature to decrease the crystallization rate for PVDF composites. The negative effect on growth rate is stronger than the positive effect on nucleating for the crystallization rate, the spherulitic growth rate dominates the crystallization process, and the overall crystallization rates of PVDF composites are slower than that of PVDF. The value of Z_c for PVDF/IL is the smallest because the interaction between the $>CF_2$ group and IL restrain segmental motion at low temperature and helpful to the formation of the all-trans conformation. So the PVDF/0.5IL/0.5Gra can use the effect of nucleation of IL and Gra, and restrain segmental motion to form β phase at different cooling rate.

Vyazovkin suggested the cooling process should be studied by the isoconversional method.[49] Doyle gave easy form of the equation according to the isoconversional method, which was put forward by Flynn, Wall and Ozawa.[50-52]

$$\log \Phi = \log\left(\frac{AE_a}{RG(\alpha)}\right) - 2.315 - 0.4567\frac{E_a}{RT} \qquad (8)$$

Where, G(α) is the integral form of crystallization mechanism function, A is a pre-exponential factor, and (log (AE_a/RG(α))) is a constant.

Fig. 9 shows the FWO plots for all samples at various conversions. T_p corresponds to the temperature of current relative crystallinity. The activation energy can be calculated by the slope of fitting line. Fig. 10 shows plots of the activation energies, E_a, as a function of X_t at different conversion. All values are negative, and activation energy is reduced with increasing of relative crystallinity, the slope of curves expresses the change rate of activation energy with relative crystallinity. The value of E_a for PVDF is the biggest, and the value of E_a for PVDF/1IL is the smallest at same relative crystallinity. When the relative crystallinity between 20% - 60%, the activation energy is around the same value of the sample with IL, this appearance indicates the β crystal is so small. After finishing the nucleation task, β crystal take up few energy between process of growth. But the growth of α crystal spent more time, and suffer the extrusion from β crystal, so the energy carves become much steeper at secondary crystallization. In the non-isothermal crystallization process, IL and Gra can support nucleating agent at higher

temperature to decrease the E_a for PVDF composites, but IL and Gra can restrain spherulitic growth at lower temperature to decrease the crystallization rate for PVDF composites. For PVDF/0.5IL/0.5Gra, IL and Gra can facilitate nucleation to decrease E_a, combined efforts of the IL and Gra can maintain appropriate crystallization rate to form β phase extruded form α phase.

4. Conclusion

In our study, IL, Gra and Gra modified by IL were incorporated in PVDF by solution mixing. The IL and Gra have different roles in this system, a kind of inducer and nucleation agent, respectively. The positive effect on the crystallization of PVDF may be ascribed to Gra-imidazolium cation and $>CF_2$-imidazolium cation interactions during isothermal crystallization. In the non-isothermal crystallization process, the PVDF/0.5IL/0.5Gra can use the effect of nucleation of IL and Gra, and restrain segmental motion to form β phase at different cooling rate and to decrease the E_a for PVDF composites, but IL and Gra can restrain spherulitic growth at lower temperature to decrease the crystallization rate for PVDF composites. Energy carves show that β crystal is smaller and grows faster. While the growth of α crystal spent more time, and suffer the extrusion from β crystal. In the isothermal and non-isothermal crystallization process, for PVDF/0.5IL/0.5Gra, IL and Gra can facilitate nucleation to decrease E_a, combined efforts of the IL and Gra can maintain appropriate crystallization rate to form β phase extruded form α phase.

Acknowledgments

This research was supported by the National Science Foundation of China (51373045) and the Anhui Provincial Natural Science Foundation (1308085QB40).

References

1 Y. Chen, Q. Deng, J. Mao, H. Nie, L. Wu, W. Zhou and B. Huang, *Polymer*, 2007, **48**, 7604-7613.

2 Y. C. Chiang, Y. Chang, A. Higuchi, W.-Y. Chen and R.-C. Ruaan, *J. Membr. Sci.*, 2009, **339**, 151-159.

3 Y. Yang, G. Wu, S. Ramalingam, S. L. Hsu, L. Kleiner and F. W. Tang, *Macromolecules*, 2007, **40**, 9658-9663.

4 B. Ameduri, *Chem. Rev.*, 2009, **109**, 6632-6686.

5 J. C. Wang, P. Chen, L. Chen, K. Wang, H. Deng, F. Chen, Q. Zhang and Q. Fu, *Express Polym. Lett.*, 2012, **6**, 299-307.

6 A. Kelarakis, S. Hayrapetyan, S. Ansari, J. Fang, L. Estevez and E. P. Giannelis, *Polymer*, 2010, **51**, 469-474.

7 K. P. Pramoda, A. Mohamed, I. Y. Phang and L. Tianxi, *Polym. Int.*, 2005, **54**, 226-232.

8 Z. Cui, E. Drioli and Y. M. Lee, *Prog. Polym. Sci.*, 2014, **39**, 164-198.

9 B. P. Tripathi and V. K. Shahi, *Prog. Polym. Sci.*, 2011, **36**, 945-979.

10 P. Martins, A. C. Lopes and S. Lanceros-Mendez, *Prog. Polym. Sci.*, 2014, **39**, 683-706.

11 F. Liu, N. A. Hashim, Y. T. Liu, M. R. M. Abed and K. Li, *J. Membr. Sci.*, 2011, **375**, 1-27.

12 A. Rehman and X. Q. Zeng, *Acc. Chem. Res.*, 2012, **45**, 1667-1677.

13 J.-C. Plaquevent, J. Levillain, F. Guillen, C. Malhiac and A.-C. Gaumont, *Chem. Rev.*, 2008, **108**, 5035-5060.

14 E. Ahmed, J. Breternitz, M. F. Groh and M. Ruck, *Crystengcomm*, 2012, **14**, 4874-4885.

15 X. F. Yang, N. L. Ge, L. Y. Hu, H. G. Gui, Z. G. Wang and Y. S. Ding, *Polym. Adv. Technol.*, 2013, **24**, 568-575.

16 P. Xu, H. G. Gui, S. Z. Yang, Y. S. Ding and Q. Hao, *Macromol. Res.*, 2014, **22**, 304-309.

17 L. H. He, J. Sun, X. X. Wang, C. D. Wang, R. Song and Y. M. Hao, *Polym. Int.*, 2013, **62**, 638-646.

18 C. L. Liang, Q. Xie, R. Y. Bao, W. Yang, B. H. Xie and M. B. Yang, *J. Mater. Sci.*, 2014, **49**, 4171-4179.

19 C. Y. Xing, L. P. Zhao, J. C. You, W. Y. Dong, X. J. Cao and Y. J. Li, *J. Phys. Chem. B*, 2012, **116**, 8312-8320.

20 C. Y. Xing, M. M. Zhao, L. P. Zhao, J. C. You, X. J. Cao and Y. J. Li, *Polym. Chem.*, 2013, **4**, 5726-5734.

21 D. Okada, H. Kaneko, K. Kato, S. Furumi, M. Takeguchi and Y. Yamamoto, *Macromolecules*, 2015, **48**, 2570-2575.

22 M. S. Xu, T. Liang, M. M. Shi and H. Z. Chen, *Chem. Rev.*, 2013, **113**, 3766-3798.

23 V. Georgakilas, M. Otyepka, A. B. Bourlinos, V. Chandra, N. Kim, K. C. Kemp, P. Hobza, R. Zboril and K. S. Kim, *Chem. Rev.*, 2012, **112**, 6156-6214.

24 P. Martins, C. Caparros, R. Goncalves, P. M. Martins, M. Benelmekki, G. Botelho and S.

Lanceros-Mendez, *J. Phys. Chem. C*, 2012, **116**, 15790-15794.

25 R. K. Layek, S. Samanta, D. P. Chatterjee and A. K. Nandi, *Polymer*, 2010, **51**, 5846-5856.

26 N. L. An, S. L. Liu, C. Q. Fang, R. E. Yu, X. Zhou and Y. L. Cheng, *J. Appl. Polym. Sci.*, 2015, **132**.

27 P. Han, J. B. Fan, M. X. Jing, L. Zhu, X. Q. Shen and T. Z. Pan, *J. Compos. Mater.*, 2014, **48**, 659-666.

28 L. Y. Huang, C. X. Lu, F. Wang and L. Wang, *Rsc Adv.*, 2014, **4**, 45220-45229.

29 A. P. Saxena, M. Deepa, A. G. Joshi, S. Bhandari and A. K. Srivastava, *Acs Appl. Mater. Inter.*, 2011, **3**, 1115-1126.

30 Z. Tang, L. Zhang, C. Zeng, T. Lin and B. Guo, *Soft Matter*, 2012, **8**, 9214-9220.

31 C. Zeng, Z. Tang, B. Guo and L. Zhang, *PCCP*, 2012, **14**, 9838-9845.

32 J. Lu, J.-x. Yang, J. Wang, A. Lim, S. Wang and K. P. Loh, *Acs Nano*, 2009, **3**, 2367-2375.

33 Y. Liang, D. Wu, X. Feng and K. Muellen, *Adv. Mater.*, 2009, **21**, 1679-+.

34 Y. K. Yang, C. E. He, R. G. Peng, A. Baji, X. S. Du, Y. L. Huang, X. L. Xie and Y. W. Mai, *J. Mater. Chem.*, 2012, **22**, 5666-5675.

35 B. Mohammadi, A. A. Yousefi and S. M. Bellah, *Polym. Test.*, 2007, **26**, 42-50.

36 M. Sharma, G. Madras and S. Bose, *Macromolecules*, 2014, **47**, 1392-1402.

37 M. Avrami, *J. Chem. Phys.*, 1939, **7**, 1103-1112.

38 M. Avrami, *J. Chem. Phys.*, 1941, **9**, 177-184.

39 S. K. Chaurasia, R. K. Singh and S. Chandra, *Crystengcomm*, 2013, **15**, 6022-6034.

40 X. Wang, X. Y. Zhang and L. Zhang, *J. Appl. Polym. Sci.*, 2013, **128**, 400-406.

41 H. M. Chen, X. C. Du, A. S. Yang, J. H. Yang, T. Huang, N. Zhang, W. Yang, Y. Wang and C. L. Zhang, *Rsc Adv.*, 2014, **4**, 3443-3456.

42 H. L. Guo, Y. Zhang, F. F. Xue, Z. W. Cai, Y. R. Shang, J. Q. Li, Y. Chen, Z. H. Wu and S. C. Jiang, *Crystengcomm*, 2013, **15**, 1597-1606.

43 P. Cebe and S. D. Hong, *Polymer*, 1986, **27**, 1183-1192.

44 J. Bai, H. G. Fang, Y. Q. Zhang and Z. G. Wang, *Crystengcomm*, 2014, **16**, 2452-2461.

45 H. M. Chen, W. B. Zhang, X. C. Du, J. H. Yang, N. Zhang, T. Huang and Y. Wang, *Thermochim. Acta*, 2013, **566**, 57-70.

46 J. R. Gregorio and M. Cestari, *J. Polym. Sci. Pol. Phys.*, 1994, **32**, 859-870.

47 P. Martins, C. M. Costa, M. Benelmekki, G. Botelho and S. Lanceros-Mendez, *Crystengcomm*, 2012, **14**, 2807-2811.

48 A. Jeziorny, *Polymer*, 1978, **19**, 1142-1144.

49 S. Vyazovkin and N. Sbirrazzuoli, *J. Phys. Chem. B*, 2003, **107**, 882-888.

50 C. D. Doyle, *Anal. Chem.*, 1961, **33**, 77-79.

51 J. H. Flynn and L. A. Wall, *J. Polym. Sci. Part B: Polym. Lett.*, 1967, **5**, 191-196.

52 T. Ozawa, *Bull. Chem. Soc. Jpn.*, 1965, **38**, 1881-1886.

Content of Figures and Tables

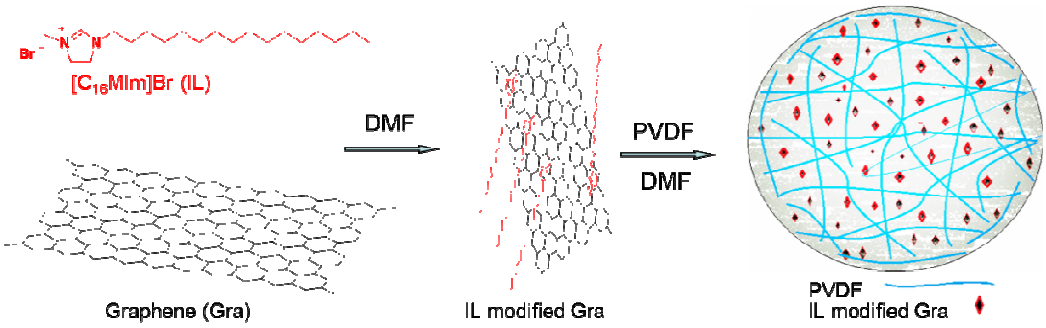

Fig. 1 Structures of IL and schematic diagram of the preparation of PVDF/IL/Gra composite

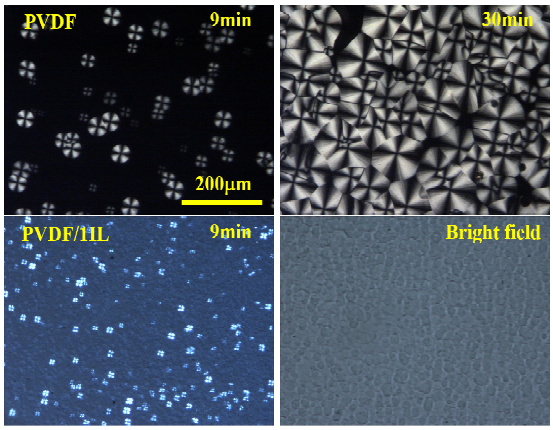

Fig. 2 POM images of samples with scale bars of 200 μm.

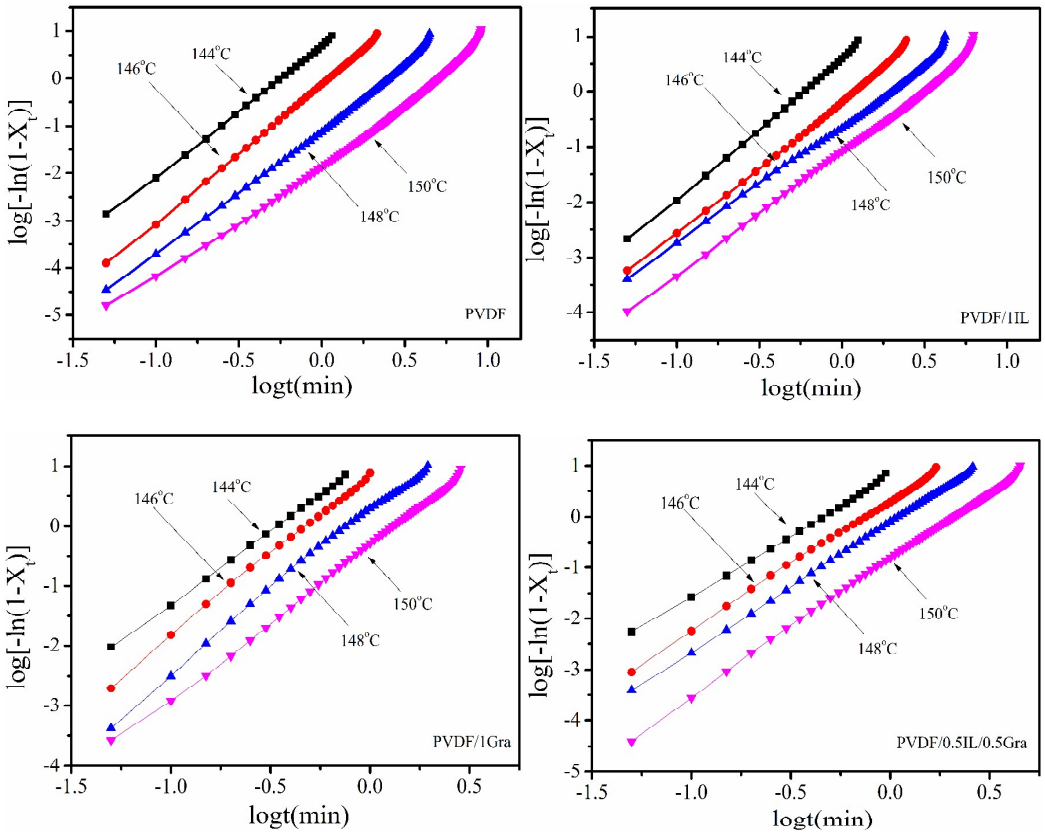

Fig. 3 Plot of (log [-ln (1-X_t)]) versus (log t) for isothermal crystallization of samples.

5

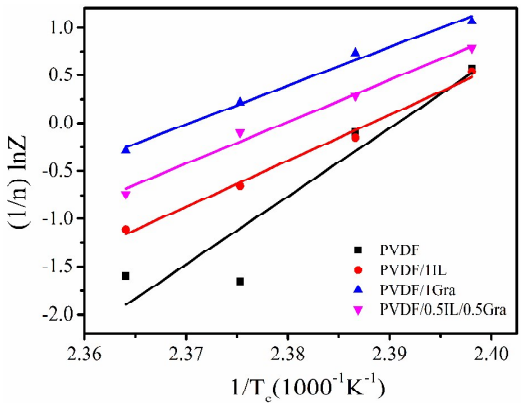

Fig. 4 Plot of $((1/n) \ln Z)$ versus $(1/T_c)$ of samples for the Avrami parameter Z deduced from isothermal crystallization.

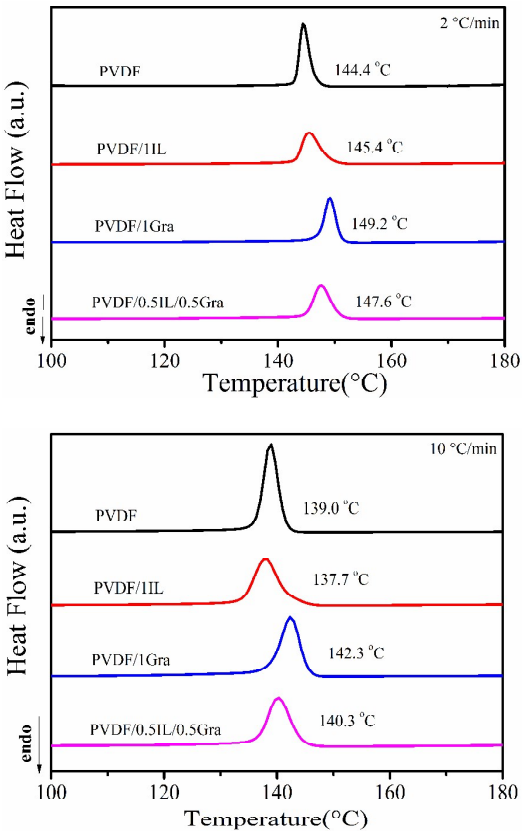

Fig. 5 First cooling DSC curves of all samples at 2 ºC/min and 10 ºC/min.

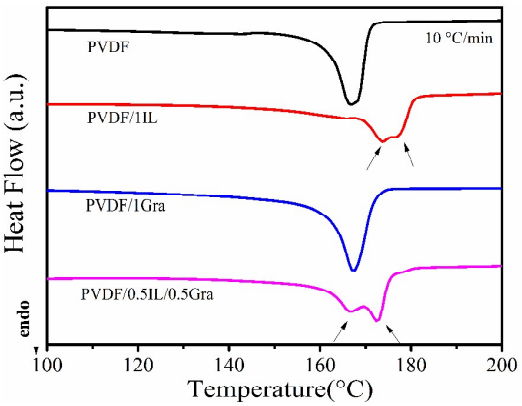

Fig. 6 Second heating DSC curves of all samples after cooling at 10 ºC/min (heating rate is 10 ºC/min).

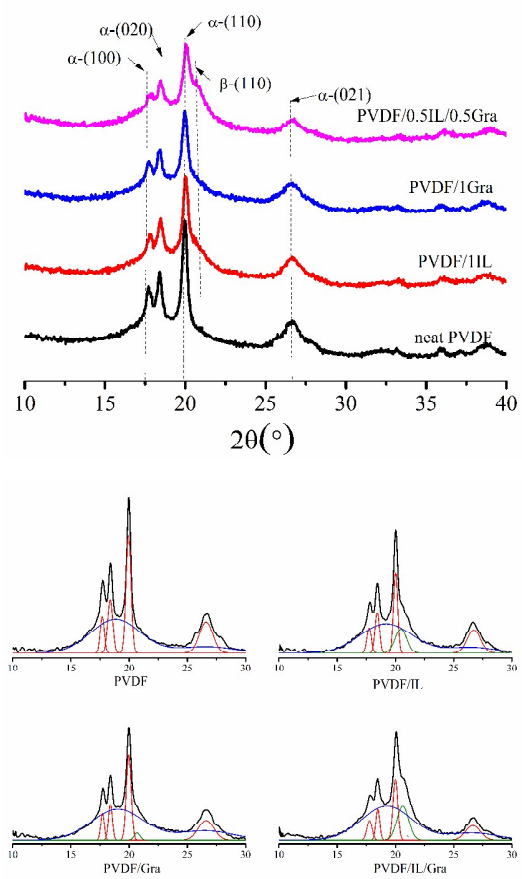

Fig. 7 XRD profiles of all samples after hot pressing and the below is peak fitting of XRD profiles of all samples. The curves are the simulated diffractions of α-phase (red), β-phase (green) and amorphous phase (blue).

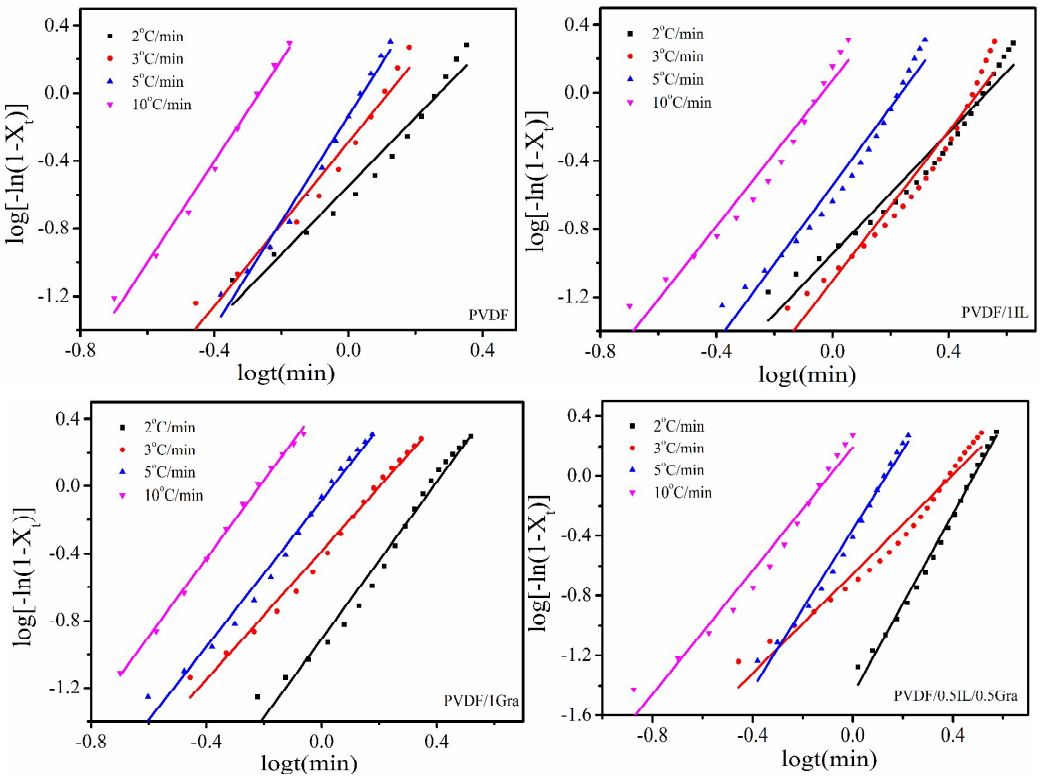

Fig. 8 Plot of (log [-ln (1-X_t)]) versus (log t) for non-isothermal crystallization of samples.

5

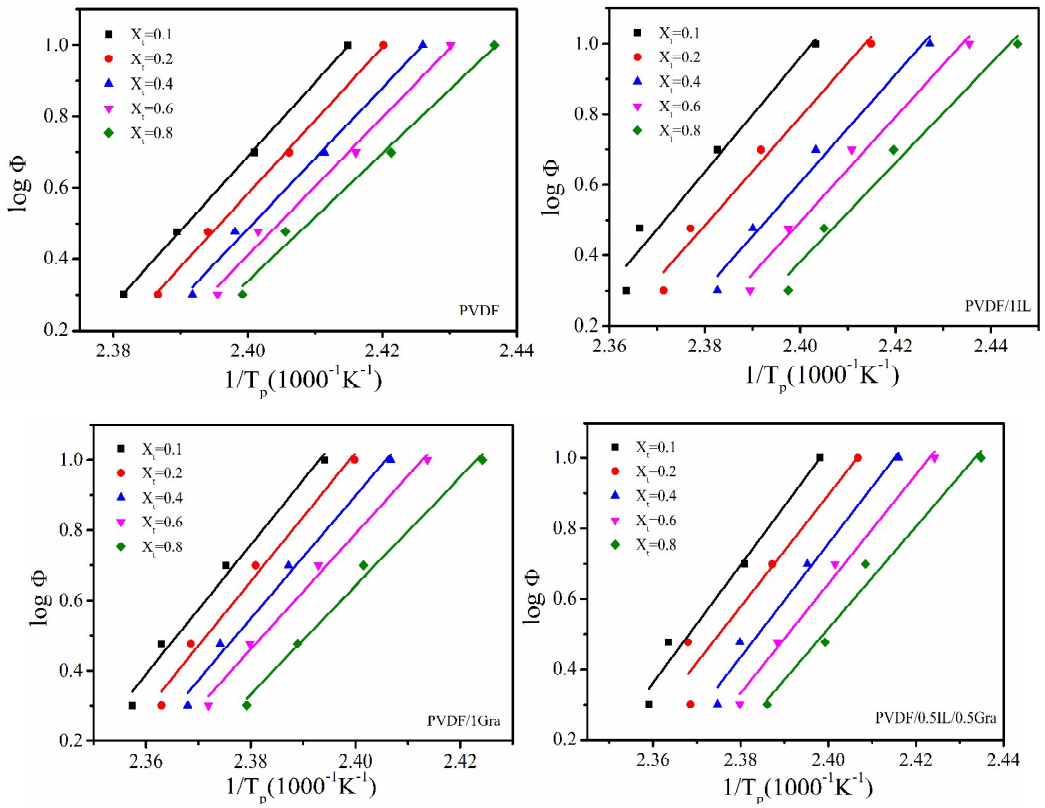

Fig. 9 FWO plots for samples at various conversions.

5

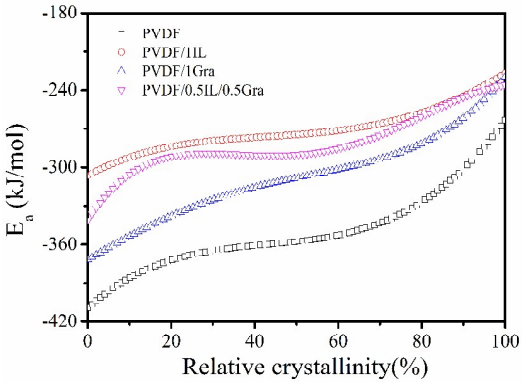

Fig. 10 Non-isothermal crystallization activation energy for PVDF and other samples.

Table 1 Composition of the PVDF, PVDF/IL, PVDF/Gra and PVDF/IL/Gra samples.

Samples	PVDF/g	IL/g	Gra/g	Ratio
PVDF	2	0	0	100/0/0
PVDF/1IL	2	0.02	0	100/1/0
PVDF/1Gra	2	0	0.02	100/0/1
PVDF/0.5IL/0.5Gra	2	0.01	0.01	100/0.5/0.5

Table 2 Parameters of isothermal crystallization from the Avrami equation.

Samples	T_c(°C)	n	log Z	$t_{1/2}$(min)	$\tau_{1/2}$(min^{-1})
PVDF	144	2.77	0.69	0.49	2.04
	146	2.95	-0.12	0.96	1.04
	148	2.75	-1.97	2.23	0.45
	150	2.65	-1.84	4.50	0.22
PVDF/1IL	144	2.56	0.60	0.50	2.00
	146	2.46	-0.16	1.02	0.98
	148	2.18	-0.62	1.73	0.58
	150	2.28	-1.10	2.76	0.36
PVDF/1Gra	144	2.44	1.13	0.29	3.45
	146	2.66	0.85	0.41	2.44
	148	2.63	0.25	0.65	1.54
	150	2.56	-0.32	1.12	0.89
PVDF/0.5IL/0.5Gra	144	2.40	0.82	0.40	2.50
	146	2.51	0.31	0.64	1.56
	148	2.52	-0.11	0.94	1.06
	150	2.62	-0.84	1.78	0.56

Table 3 Thermodynamic Parameter Got from that Curves.

Samples	T_m/°C	
PVDF	167.0	
PVDF/1IL	173.7	177.0
PVDF/1Gra	167.7	
PVDF/0.5IL/0.5Gra	167.0	172.3

Table 4 Parameters of non-isothermal crystallization from the Avrami equation.

Samples	Φ(°C • min^{-1})	2	3	5	10
PVDF	$t_{1/2}$(min)	1.61	1.15	0.99	0.49
	n	2.02	2.42	3.12	2.99
	Z_c	0.532	0.801	0.940	1.20
PVDF/1IL	$t_{1/2}$(min)	2.90	2.77	1.51	0.80
	n	1.78	2.20	2.30	2.15
	Z_c	0.336	0.428	0.778	1.017
PVDF/1Gra	$t_{1/2}$(min)	2.06	1.31	0.92	0.51
	n	2.34	1.91	2.18	2.32
	Z_c	0.351	0.744	0.962	1.12
PVDF/0.5IL/0.5Gra	$t_{1/2}$(min)	2.70	2.09	1.20	0.68
	n	2.41	1.66	2.66	2.06
	Z_c	0.347	0.605	0.849	1.05